

# Effects of plasma expansion plumes in view of pulses laser irradiating centimeter-scale spherical space debris

YINGWU FANG

Xi'an International University, Yudou Road 18, Xi'an 710077, PR China;  
yiwangfang88@163.com

The objective of this article was to investigate the dynamic evolution behaviors of plasma expansion plumes by pulses laser irradiating centimeter-scale spherical space debris. A calculated model of centimeter-scale spherical space debris irradiated by pulses laser was firstly deduced based on FEM (finite element method)/COMSOL, and the action rules of plasma expansion plumes by pulses laser-generated irradiating the debris were simulated for different laser powers and action times. The results showed that the velocity of plasma expansion plumes was increased with the increase of laser powers and action times. Especially, when the laser power was 700 kW and the action time was close to 25  $\mu\text{s}$ , the maximum velocity of plasma expansion plumes approached 1.91 km/s, and the diffusion radius of plasma expansion plumes was increased by about 2.5 mm. Further, the diffusion radius was about twice that of 400 kW when the action time reached about 48  $\mu\text{s}$ . As a result, by simulating the transient flow process of nanosecond pulses laser irradiating small spherical space debris, the flow field evolution information and plasma plumes evolution characteristics of centimeter-scale space debris at nanosecond time resolution were revealed.

Keywords: plasma expansion plumes, pulse laser, centimeter-scale spherical space debris, dynamic model.

## 1. Introduction

At present, there are thousands of satellites in orbit. However, most of these satellites operate in a dense area of space debris, and the risk of collision with space debris is very high [1, 2]. For instance, a piece of space debris knocked out a visible hole in the international space station's (ISS) robotic arm, and damaged the thermal-protective coating and arm lever. There are 34000 visible impact craters on the long duration exposed facility (LDEF) of NASA. Figure 1 showed the real scene of impact cases for ISS and LDEF [3, 4]. Therefore, the effective management of space debris is an important issue that must be resolved as soon as possible.

Generally, centimeter-scale space debris is classified as small debris materials. Relevant studies show that active removal of centimeter-scale space debris is one of the most promising methods by pulse laser irradiation [5, 6]. Laser removal of centimeter

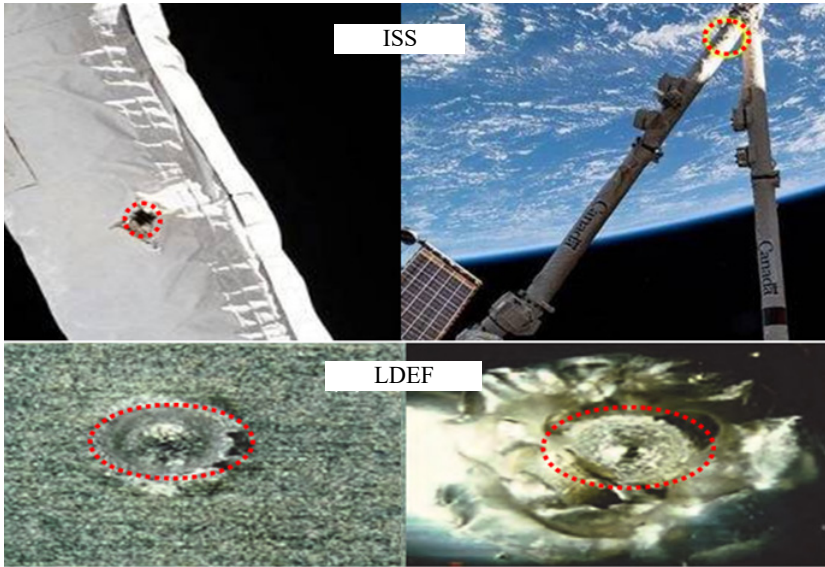


Fig. 1. The impact cases of ISS and LDEF.

-scale space debris is affected by many factors including laser parameters, physical parameters and geometric parameters of different materials, *etc.* PHIPPS found that action rules of impulse coupling coefficient of planar space debris are joined with laser power density by pulse laser irradiation [7]. SHEN *et al.* carried out experimental research on laser ablation expansion plume for typical materials of space debris [8]. TRAN *et al.* analyzed the impulse and mass removal rate of aluminum space debris by nanosecond laser ablation in a wide range of ambient pressure [9]. CICHOCKI *et al.* investigated the interaction between a spacecraft, a plasma thruster plume and a free floating object, in the context of an active space debris removal mission based on the ion beam shepherd concept [10]. CHEN *et al.* discussed the influence of different geometry shapes of space debris for laser impulse, and presented a new method for calculating the impulse magnitude and direction for the irregular debris [11]. LAPUSHKINA *et al.* described the interaction of a plane shock wave with an area of ionization instability of discharge plasma in air, and demonstrated the flow modes with the disappearance of the shock wave front caused by the origin of a structure with cellular order of shear layer instabilities [12]. ZHOU *et al.* investigated an ablation impulse irradiated by nanosecond laser with aluminum planar and sphere space debris in a large beam spot [13]. Moreover, the authors are also carrying out the flow field properties and active deorbit process of different debris materials irradiated by high energy pulses laser [14, 15]. Generally, scholars at home and abroad are actively carrying out theoretical and experimental research on laser irradiation of space debris.

Space debris belongs to hypervelocity non-cooperative moving target, and it is difficult to accurately understand the characteristics of plasma expansion plumes irradiated by high-energy pulsed laser through experiments. In order to systematically grasp

the dynamic behaviors of the plasma expansion plumes when pulses laser irradiates the debris, the dynamic evolution mechanism of pulses laser irradiating the debris still needs to be further studied. Hence, the main aim of this article is to investigate the action rules of plasma expansion plumes by numerical simulations, and reveal the formation characteristics of recoil impulse and the flow fields of plasma expansion plumes through pulses laser-generated irradiating centimeter-scale spherical space debris. The research results will provide an important theoretical reference for the engineering application of space debris removal.

## 2. Analysis of model

The main components of space debris include aluminum/aluminum alloy, composite materials, stainless steel, titanium alloy and copper, among which the proportion of aluminum/aluminum alloy is more than 44%. The main geometric shapes of space debris are plate, block, rod and sheet, but most of them are irregular. In this article, the sphere debris of aluminum alloy material will be selected to establish the dynamic model irradiated by pulses laser. When the pulses laser irradiates the debris surface, vaporization and ionization occur in the irradiation zone of debris surface. Finally, the high temperature and high pressure plasma and gaseous matter are splashed to form the plasma expansion plumes, and the action process of laser irradiation is given, as shown in Fig. 2.

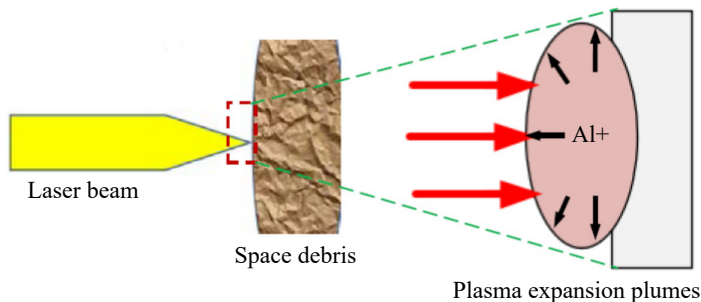


Fig. 2. The action process by laser irradiation.

When the laser power reaches a certain threshold, the surface of the debris begins to be vaporized, and the initial condition is given as follows:

$$T = T_a, \quad P = P_a, \quad n_v = 0, \quad v = 0 \quad (1)$$

where  $T_a$  denotes the initial ambient temperature,  $P_a$  denotes the initial ambient pressure,  $n_v$  denotes the vapour density, and  $v$  denotes the initial velocity.

Further, the debris material is ionized to form a high temperature and high pressure plasma expansion plumes when the pulse laser energy is close to  $10^9$  kW/cm<sup>2</sup> for the aluminum alloy, and the corresponding expression is given as follows [16]:

$$\rho_1 C \left( \frac{\partial T}{\partial t} - u(t) \right) \frac{\partial T}{\partial x} = \frac{\partial}{\partial x} \left( k_s \frac{\partial T}{\partial x} \right) + Q(x, t), \quad t_1 < t < \tau \quad (2)$$

where  $\rho_1$  denotes the liquid material density of the debris,  $C$  denotes the specific heat of the debris,  $k_s$  denotes the heat conductivity coefficient of the debris,  $\tau$  denotes the laser pulse width, and  $Q$  denotes the laser energy emitted by the laser.

Then, the initial condition can be given when the laser shot is in the  $z$ -direction:

$$T(z, t_1) = T(t_1) \quad (3)$$

The corresponding boundary condition is also expressed as

$$\begin{cases} -k_s \frac{\partial T}{\partial z} \Big|_{z=0} = Q_s(t) - \rho_1 [L_m u_m + L_v u(t)] \\ -k_s \frac{\partial T}{\partial z} \Big|_{z=l} = 0 \end{cases} \quad (4)$$

where  $Q_s$  is the laser energy incident on the debris surface,  $z$  is the distance from the incident laser direction to the debris surface,  $L_m$  is the latent heat of fusion of the debris,  $L_v$  is the latent heat of vaporization of the debris,  $u_m$  is the melting rate of the surface material of the debris,  $u(t)$  is the vaporization rate of the surface material of the debris, and  $l$  is the thickness of the debris.

Considering the plasma as a fluid and ignoring viscosity and heat conduction, the governing equation describing the expansion motion of the vapor plasma on the debris surface is simplified as [17]

$$\begin{cases} \frac{\partial \rho_1}{\partial t} + \frac{\partial \rho_1 v_1}{\partial z} = 0 \\ \frac{\partial \rho_1 v_1}{\partial t} + \frac{\partial (P_1 + \rho_1 v_1^2)}{\partial z} = 0 \\ \frac{\partial (E + 0.5 \rho_1 v_1^2 + P_1)}{\partial z} + \frac{\partial (E + 0.5 \rho_1 v_1^2)}{\partial t} + QI(z, t) = 0 \end{cases} \quad (5)$$

where  $E$  represents the internal energy per unit volume,  $I(z)$  represents the power density along the laser incident direction,  $P_1$  represents the plasma pressure, and  $v_1$  represents the velocity of the plasma splashing direction.

In the process of plasma ejection, the interaction between the plasma plumes and the debris will make the debris gain a certain speed. However, the debris velocity is mainly related to the action efficiency of the debris irradiated by pulses laser, that is,

the impulse coupling coefficient. For the debris of aluminum material, the expression of impulse coupling coefficient can be simplified as [18]:

$$C_m = 5.56 (I\lambda\sqrt{\tau})^{-0.301} \quad (6)$$

where  $\lambda$  denotes the laser wavelength, and  $C_m$  denotes the impulse coupling coefficient.

By analyzing the interaction process between pulses laser and different materials, the laser energy density and pulse width meet the approximate relationship based on the optimal impulse coupling condition [5, 14].

$$\Phi_{\text{opt}} \approx B\sqrt{\tau} \quad (7)$$

where  $\Phi_{\text{opt}}$  denotes the optimal density of laser energy,  $B$  is suitable for laser pulse widths ranging from 100 ps to 1 ms under vacuum conditions, and  $B = 8.5 \times 10^8 \text{ J/m}^2$ .

Further, after the pulse width is given, the optimal power density can be obtained according to Eq. (7):

$$I_{\text{opt}} \approx 8.5 \times 10^8 \tau^{-0.5} \quad (8)$$

where  $I_{\text{opt}}$  denotes the optimal power density of incident laser.

When strong laser pulses are irradiating the debris, the dynamic mechanism plays a decisive role in the coupling performance between laser and debris, and the dynamic equation of impulse transfer is expressed as follows [19]:

$$m\Delta v = \eta C_m I k J \quad (9)$$

where  $\Delta v$  is the velocity increment obtained by the debris,  $k$  is the irradiation direction of incident laser,  $J$  is the second-order area matrix of the debris, and  $\eta$  is the efficiency factor.

Assuming the laser spot is completely irradiated on the debris surface, and all the laser energy is absorbed, the velocity increment of the debris can be obtained as follows:

$$\Delta v = \frac{\eta C_m I k J}{m} \quad (10)$$

As a result, the corresponding dynamic model irradiated by pulses laser is established by combining Eqs. (6) and (8) to Eq. (10). Especially, the efficiency factor is equal to 1 in the process of numerical simulations.

Based on the above analysis, the following step will investigate the dynamic evolution behaviors of plasma expansion plumes by numerical simulations. In the process of numerical calculations, the laser action times refer to the time that the pulsed laser irradiates the debris, and includes the time of pulse interval. Relevant theoretical studies show that a single pulse of laser energy cannot achieve excellent effect, and the

continuous action of multiple pulses laser is needed. Hence, according to the Kepler equation, the time of pulse interval should be considered in the process of multi-pulse laser irradiating materials.

### 3. Model and simulation platform

As an example, a kind of centimeter-scale spherical space debris materials including aluminum and aluminium alloy was selected to investigate the dynamic characteristics of plasma expansion plumes. Suppose the radius of sphere debris was 0.01 m and the density was  $2700 \text{ kg/m}^3$ , and the main simulated parameters were shown in the Table. The following established the simulation model including the geometric model and the corresponding calculated model of the debris.

T a b l e. List of the main simulated parameters.

Heat capacity at constant pressure	Elasticity modulus	Poisson's ratio	Laser frequency repetition	Laser wavelength	Laser pulse width
$900 \text{ J}\cdot(\text{kg}\cdot\text{K})^{-1}$	$7 \times 10^{10} \text{ Pa}$	0.33	100 Hz	1064 nm	100 ns

Based on the given parameters, the geometric model of sphere debris irradiated by pulses laser was established, as shown in Fig. 3. In the model, it was assumed that the debris was uniform and isotropic, and the change of viscous resistance during laser action was ignored.

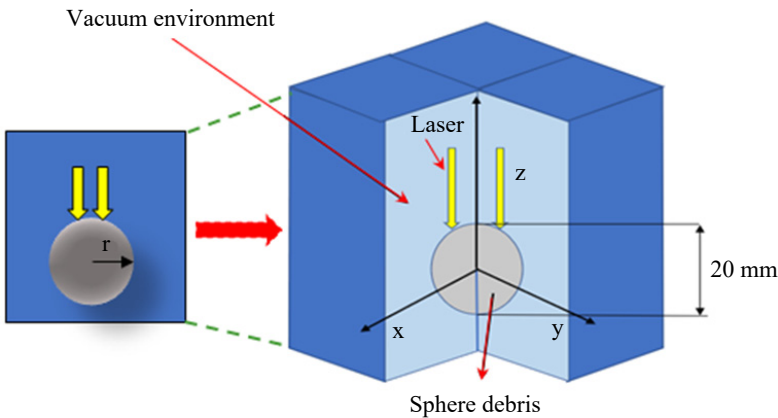


Fig. 3. The geometric model.

According to the calculation accuracy of each unit, the grid was automatically divided, and the grid size and node number were also generated by finite element method (FEM) meshing module. In order to improve the calculation accuracy and efficiency, tetrahedral elements were used in the vacuum region, and the prismatic elements were applied to the debris model. Finally, a total of 274248 tetrahedral elements

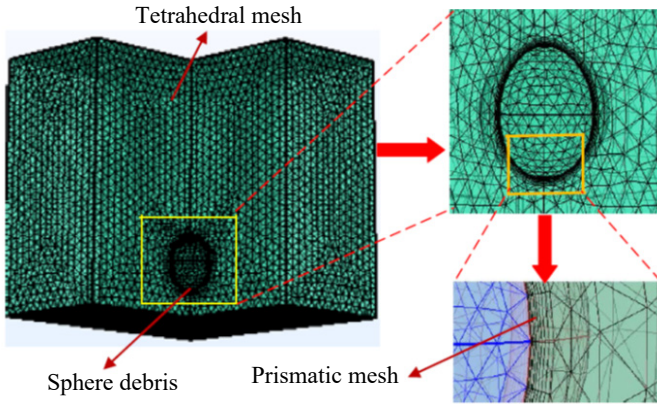


Fig. 4. The calculated model.

and 6720 prismatic elements were divided during the simulation, and the corresponding calculated model was also established by FEM. In Fig. 4, the calculated model was divided into many grids of calculating unit.

Due to the advantages of COMSOL in dealing with the coupling problem of multiple physical fields, the interaction physical process of space debris irradiated by pulses laser was simulated based on COMSOL platform in this article. As a result, a simulation platform of computing plasma expansion plumes was built by COMSOL, and the corresponding simulation interface was established, as shown in Fig. 5.

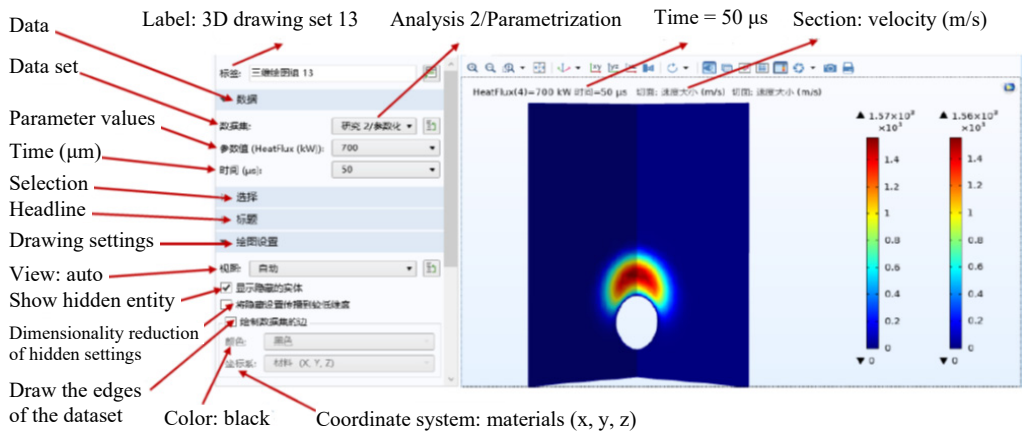


Fig. 5. The simulation interface.

### 4. Calculational examples

The interaction between high-energy pulses laser and space debris is the theoretical basis of removing the debris. Therefore, the velocity of plasma expansion plumes formed on the debris with different laser powers was investigated, and the velocity dis-

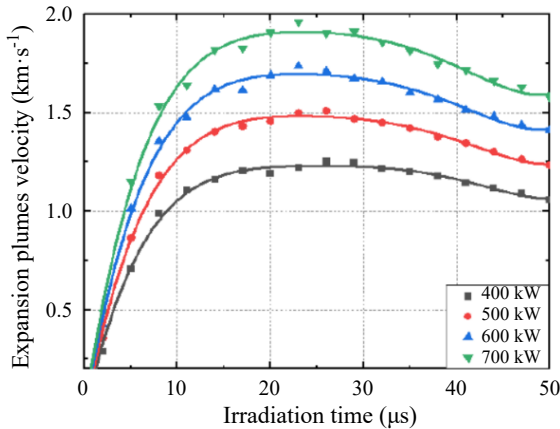


Fig. 6. The velocity curves of different laser powers.

tribution rules of plasma expansion plumes under different laser powers was analyzed. By numerical simulation, the velocity distribution characteristics of plasma expansion plumes were obtained when the incident laser power was 400, 500, 600, and 700 kW, respectively. Figure 6 shown the change curves of plasma expansion plumes velocity for different laser powers.

According to Fig. 6, with the increase of pulses laser power, the velocity of plasma expansion plumes was increased continuously. But, the velocity of plasma expansion plumes was close to the maximum value around 25  $\mu\text{s}$ . Subsequently, due to the influence of the plasma shielding effect, the velocity of plasma expansion plumes was decreased with the increase of laser power, and tended to be stable around 48  $\mu\text{s}$ . Therefore, by increasing the laser power, the interaction between the pulse laser and the debris could be improved, which could generate a larger plasma expansion plumes velocity. However, in order to effectively improve the utilization efficiency of laser energy, the plasma shielding effect needed to be considered comprehensively.

On the basis of the above results, when the action times were 25 and 48  $\mu\text{s}$ , the evolution rules of plasma expansion plumes were investigated based on different incident laser powers. Assuming the incident laser power was 400, 500, 600, and 700 kW, the evolution plots of plasma expansion plumes formed by pulses laser irradiating the debris were obtained during the action times of 25 and 48  $\mu\text{s}$ , as shown in Figs. 7 and 8.

By analyzing the evolution plots in Figs. 7 and 8, it was found that the arc-shaped distribution zone of plasma expansion plumes was significantly increased with the increase of laser powers. Especially, compared with 400 kW, the diffusion radius of plasma expansion plumes generated at 700 kW was increased by about 2.5 mm when the action time was 25  $\mu\text{s}$ . However, when the action time reached 48  $\mu\text{s}$  or so, the diffusion radius of 700 kW was about twice that of 400 kW, and the velocity of plasma expansion plumes dropped to 1.63 km/s. Subsequently, due to the plasma shielding effect,



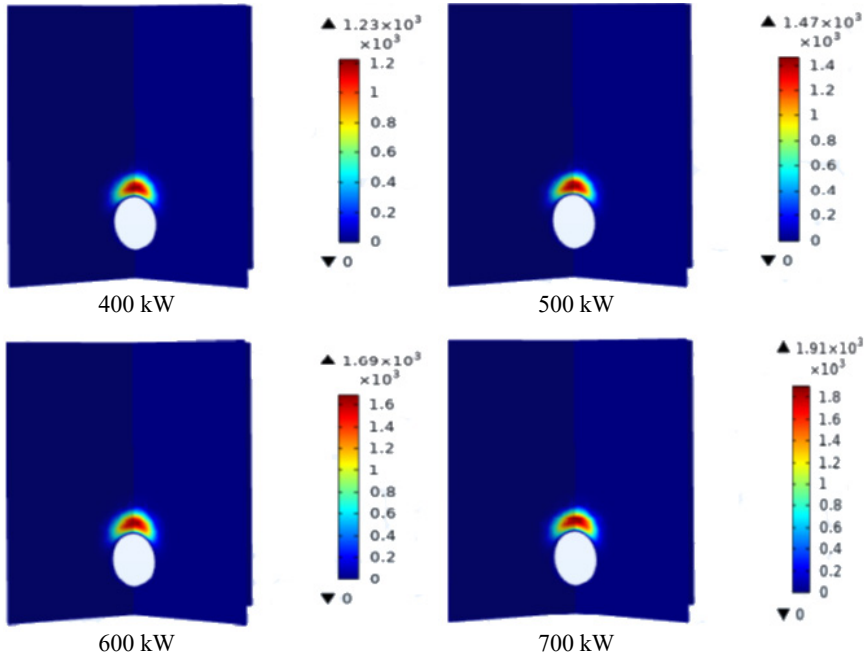


Fig. 7. The evolution plots during 25  $\mu$ s.

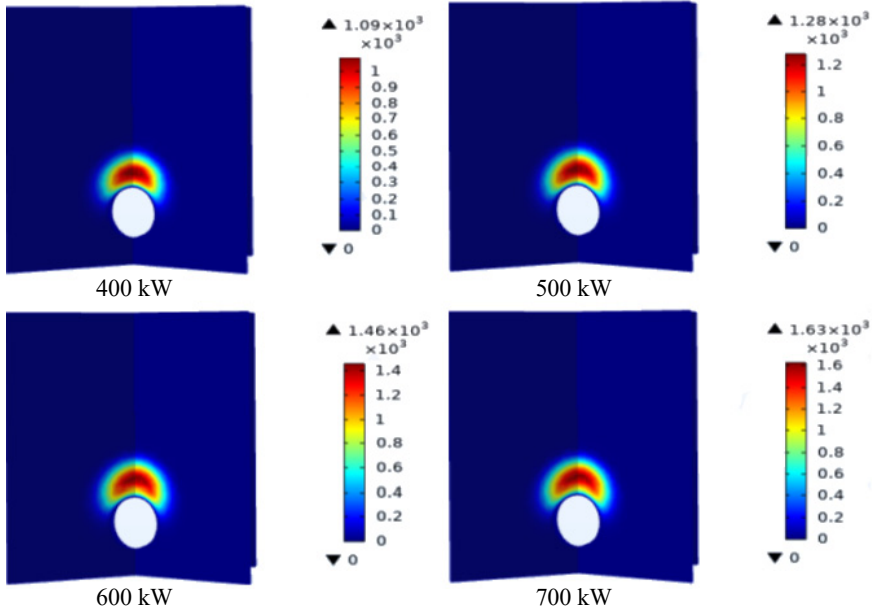


Fig. 8. The evolution plots during 48  $\mu$ s.

the plasma expansion plumes gradually became stable. Thus, the laser power of 700 kW had a very obvious advantage in improving the optimal efficiency of plasma expansion plumes.

The above study preliminarily revealed the evolution rules of plasma expansion plumes based on different pulses laser power. However, the action time of pulses laser is also critical to the transient distribution of plasma expansion plumes. Further, when the laser power was 700 kW, the following discussed the distribution rules of plasma

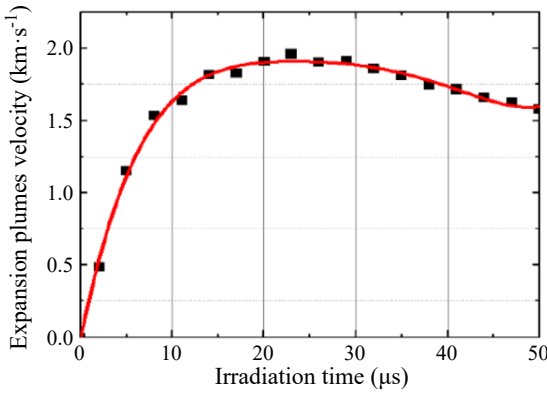


Fig. 9. The velocity curve of different action times.

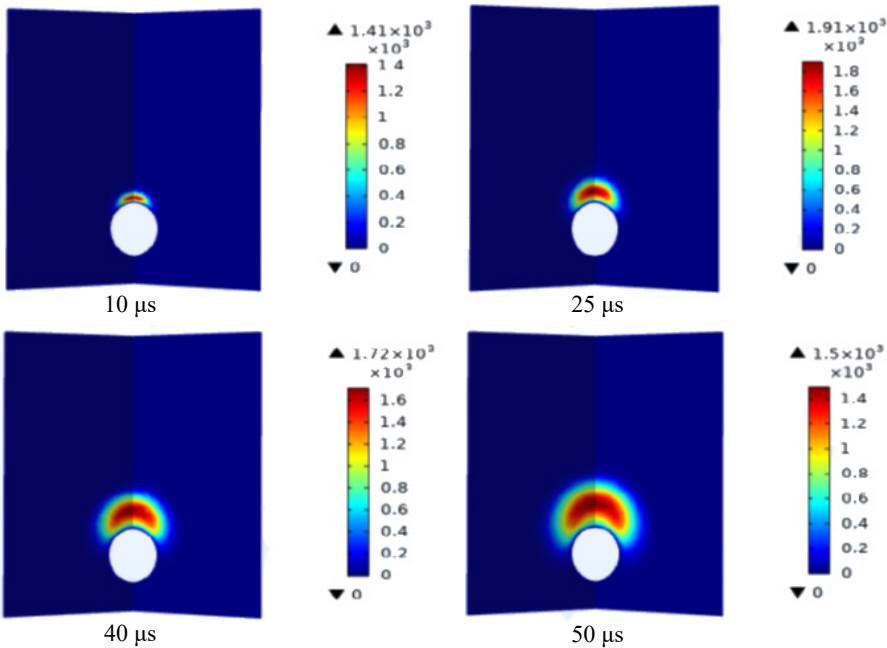


Fig. 10. The evolution plots during 700 kW.

expansion plumes based on different action times. By numerical simulation, the velocity change curve of plasma expansion plumes under different action times was computed, as shown in Fig. 9. At the same time, Fig. 10 emerged the evolution plots of plasma expansion plumes when the action time was 10, 25, 40, and 50  $\mu\text{s}$ , respectively.

By comparing the simulation results in Figs. 9 and 10, it was found that the maximum velocity of plasma expansion plumes was rapidly increased when the pulses laser irradiated the debris surface. Especially, the maximum velocity of plasma expansion plumes was the highest along the laser incident direction, and the plasma expansion plumes were continued to spread outwards within a certain irradiation times. When the action time was close to 25  $\mu\text{s}$ , the maximum velocity of plasma expansion plumes reached 1.91 km/s. Then, the velocity tended to be stable before 29  $\mu\text{s}$ , and presented a downward trend after 29  $\mu\text{s}$ . Finally, the velocity remained basically unchanged after 48  $\mu\text{s}$ . This was mainly due to the dynamic pressure formed by the plasma shock waves surface and the surrounding gas. As a result, the density was decreased faster in the plasma region farther from the debris surface, and the shielding effect of plasma expansion plumes was also formed from 29 to 48  $\mu\text{s}$ . Comprehensive comparison of the results further verifies the validity of the conclusions in this article.

## 5. Conclusions

The dynamic characteristics of space debris irradiated by high-energy pulses laser depend on the evolution process of plasma expansion plumes. For centimeter-scale spherical space debris materials, the evolution rules of transient plasma plumes fields under different laser parameters were further addressed in this article. The following conclusions were drawn.

1) According to the physical interaction process of centimeter-scale spherical debris irradiated by nanosecond pulses laser, the simulation model irradiated by pulses laser was deduced based on FEM, and the corresponding simulation interface of analyzing the plasma expansion plumes was effectively established by COMSOL. The debris irradiation process was combined with the plasma expansion plumes process by setting reasonable conditions, and the established model more comprehensively reflected the evolution process of transient plasma expansion plumes fields at higher laser energy.

2) Using the calculation conditions of this paper, when the action time was close to 25  $\mu\text{s}$ , the velocity of plasma expansion plumes achieved 1.91 km/s for the laser power of 700 kW. Further, the diffusion radius of plasma expansion plumes generated at 700 kW was increased by about 2.5 mm when the action time was 25  $\mu\text{s}$ , while the diffusion radius of 700 kW was about twice that of 400 kW when the action time reached about 48  $\mu\text{s}$ . At this moment, the velocity of plasma expansion plumes dropped to 1.63 km/s.

3) During the entire irradiation period of pulses laser, the velocity of plasma expansion plumes was the highest along the laser incident direction. In particular, the velocity of plasma expansion plumes was increased with the increase of laser powers based on

the same action times. Moreover, the velocity of expansion plumes was also increased with the increase of action times based on the same laser power. However, the plasma shielding effect was still very significant for the evolution process of forming plasma expansion plumes.

### Acknowledgements

This work was funded by the National Natural Science Foundation of China (Grant No. 61875231). The author fully appreciates the financial support.

### References

- [1] SONG B., LI K., TANG H.W., *Recent developments in foreign space debris removal*, Space International **509**, 2021: 14-19.
- [2] BELKIN S.O., KUZNETSOV E.D., *Orbital flips due to solar radiation pressure for space debris in near-circular orbits*, Acta Astronautica **178**, 2021: 360-369. <https://doi.org/10.1016/j.actaastro.2020.09.025>
- [3] LI M., GONG Z.Z., LIU G.Q., *Frontier technology and system development of space debris surveillance and active removal*, Chinese Science Bulletin **63**(25), 2018: 2570-2591. <https://doi.org/10.1360/N972017-00880>
- [4] MARK C.P., KAMATH S., *Review of active space debris removal methods*, Space Policy **47**, 2019: 194-206. <https://doi.org/10.1016/j.spacepol.2018.12.005>
- [5] PHIPPS C., LUKE J., FUNK D., MOORE D., GLOWNIA J., LIPPERT T., *Laser impulse coupling at 130 fs*, Applied Surface Science **252**(13), 2006: 4838-4844. <https://doi.org/10.1016/j.apsusc.2005.07.079>
- [6] LEVCHENKO I., BARANOV O., FANG J.H., CHERKUN O., XU S.Y., BAZAKA K., *Focusing plasma jets to achieve high current density: Feasibility and opportunities for applications in debris removal and space exploration*, Aerospace Science and Technology **108**, 2021: 106343. <https://doi.org/10.1016/j.ast.2020.106343>
- [7] PHIPPS C.R., *A laser-optical system to re-enter or lower low Earth orbit space debris*, Acta Astronautica **93**, 2014: 418-429. <https://doi.org/10.1016/j.actaastro.2013.07.031>
- [8] SHEN S.Y., JIN X., LI Q., *Laser ablation expansion plume performance experiments with typical material of orbital debris*, High Power Laser and Particle Beams **27**(5), 2015: 051014. <https://doi.org/10.11884/HPLPB201527.051014>
- [9] TRAN D.T., YOGO A., NISHIMURA H., MORI K., *Impulse and mass removal rate of aluminum target by nanosecond laser ablation in a wide range of ambient pressure*, Journal of Applied Physics **122**(23), 2017: 233304. <https://doi.org/10.1063/1.5005584>
- [10] CICHOCKI F., MERINO M., AHEDO E., *Spacecraft-plasma-debris interaction in an ion beam shepherd mission*, Acta Astronautica **146**, 2018: 216-227. <https://doi.org/10.1016/j.actaastro.2018.02.030>
- [11] CHEN C., GONG Z.Z., YANG W.L., *et al.*, *Influence of geometry of space debris on laser ablation impulse*, Chinese Journal of High Pressure Physics **32**(4), 2018: 040101.
- [12] LAPUSHKINA T.A., EROFEEV A.V., AZAROVA O.A., KRAVCHENKO O.V., *Interaction of a plane shock wave with an area of ionization instability of discharge plasma in air*, Aerospace Science and Technology **85**, 2019: 347-358. <https://doi.org/10.1016/j.ast.2018.12.020>
- [13] ZHOU W.J., CHANG H., YE J.F., LI N.L., *Impulse of planar and sphere target by nanosecond laser ablation in a large beam spot*, Laser Physics **30**(6), 2020: 066002. <https://doi.org/10.1088/1555-6611/ab84e0>
- [14] FANG Y.W., *Dynamic deorbit of small-sized space debris in near-Earth orbit in view of space-based pulse laser*, Journal of Laser Applications **34**(2), 2022: 022018. <https://doi.org/10.2351/7.0000662>
- [15] FANG Y.W., PAN J., LUO Y.J., C.W. LI, *Effects of deorbit evolution on space-based pulse laser irradiating centimeter-scale space debris in LEO*, Acta Astronautica **165**, 2019: 184-190. <https://doi.org/10.1016/j.actaastro.2019.09.010>

- [16] ALI M., HENDA R., *Modeling of plasma expansion during pulsed electron beam ablation of graphite*, MRS Advances **2**, 2017: 905-911. <https://doi.org/10.1557/adv.2017.83>
- [17] SONG L.H., WEI Q., BAI Y., GAO C., *Impact effects on fused quartz glass by ground simulating hypervelocity space debris*, Science China Technological Sciences **56**(3), 2013: 724-731. <https://doi.org/10.1007/s11431-012-5126-9>
- [18] PHIPPS C.R., TURNER T.P., HARRISON R.F., YORK G.W., OSBORNE W.Z., ANDERSON G.K., CORLIS X.F., HAYNES L.C., STEELE H.S., SPICOCHI K.C., KING T.R., *Impulse coupling to targets in vacuum by KrF, HF, and CO<sub>2</sub> single-pulse lasers*, Journal of Applied Physics **64**(3), 1988: 1083-1096. <https://doi.org/10.1063/1.341867>
- [19] LIEDAHL D.A., RUBENCHIK A., LIBBY S.B., NIKOLAEV S., PHIPPS C.R., *Pulsed laser interactions with space debris: Target shape effects*, Advances in Space Research **52**(5), 2013: 895-915. <https://doi.org/10.1016/j.asr.2013.05.019>

*Received September 20, 2022  
in revised form December 22, 2022*